X-551-69-52

PREPRINT

NASA TM X-63490

EFFECT OF SATELLITE SPIN ON EXPLORER 33 AND 35 DOPPLER TRACKING DATA

J. W. MARINI
C. W. MURRAY, JR.

FEBRUARY 1969

GODDARD SPACE FLIGHT CENTER
GREENBELT, MARYLAND

X-551-69-52
Preprint

EFFECT OF SATELLITE SPIN ON EXPLORER 33 AND 35 DOPPLER TRACKING DATA

J. W. Marini
C. W. Murray, Jr.

February 1969

Goddard Space Flight Center
Greenbelt, Maryland

EFFECT OF SATELLITE SPIN ON EXPLORER 33 AND 35 DOPPLER TRACKING DATA

J. W. Marini
C. W. Murrary, Jr.

ABSTRACT

Tracking data obtained by the Goddard Range and Range Rate Tracking Stations from Explorer 33 and 35 Satellites is analyzed.

The residuals of the range rate data contain periodicities related to the spin of the satellites and the data sampling rate. Analysis of the satellite antenna indicates that the periodicities are caused by variations in the phase pattern of the antenna, which can also produce a fixed bias in the range-rate measurement.

Using a non-linear model the spin rate can be determined from the data. For the two examples given in the report, the rms of the residuals from the non-linear model is reduced by a factor of 1/2 and 1/3 compared to the rms of the residuals from a least squares straight line fitted to the same data.

CONTENTS

EFFECT OF SATELLITE SPIN ON EXPLORER 33 AND 35 DOPPLER TRACKING DATA

SUMMARY

Tracking data obtained by the Goddard Range and Range Rate Tracking Stations from Explorer 33 and 35 Satellites is analyzed. Both satellites are spin stabilized and employ a canted turnstile antenna.

The range rate data are recorded at the sampling frequency of one measurement per second. Each measurement consists of the time (approximately a half second) required to count a fixed number of cycles of the difference between the received and transmitted frequencies (plus a fixed reference frequency). The data is consequently a measure of the total change in frequency in the round trip of the signal from the ground station through the satellite and back. The two-way Doppler shift produces a slowly-varying contribution to this total change in frequency. When this contribution is removed by fitting a smooth curve (a straight line) to the data, the residuals contain periodicities which can be attributed to beat frequencies between the harmonics of the satellite spin rate and multiples of the sampling frequency.

Using a simple model for the satellite antenna configuration, it is shown that the appearance of the harmonics is caused by the presence of the same harmonics in the phase pattern of the antenna. The analysis also shows that the satellite spin can cause a constant contribution to the total frequency change measured which would appear as a fixed error in the Doppler frequency calculated.

The spin rate can also be determined by fitting the data, in a least squares sense, with a linear term plus sinusoidal terms. The fundamental sinusoidal frequency extracted is the satellite spin rate. This spin rate determination agreed to within 0.2% of that examined from references 2, 3, 6, and 7. The accuracy to which the spin rate can be determined in this manner is a function of the number of data points, the assumed model, and the short term fluctuations on the data (Appendix C). By subtracting this non-linear model from the raw data, residuals are reduced by as much as 70% relative to that obtained by a linear fit. Thus an error model of this form when subtracted from the raw tracking data will result in a reduction in the uncertainty of the computed orbit.

INTRODUCTION

Spin stabilization is one of the methods for controlling the attitude of a satellite, i.e., its orientation with respect to some reference frame. By this technique, one of the body axes is fixed in inertial space while the satellite rotates around it.

Explorer 33 (AIMP-D) and Explorer 35 (AIMP-E) are both spin stabilized for attitude control.

Explorer 33 was launched 1 July 1966. For the data epochs considered in this report, the satellite was in an elliptical orbit about the earth with the orbital parameters varying rapidly due to lunar perturbation. In general, the orbital parameters remained within the following bounds (references 1 and 2).

Perigee radius: 20,000 km to 130,000 km
Apogee radius: 400,000 km to 530,000 km

Explorer 35 was launched 19 July 1967 and is in an elliptic orbit about the moon with an aposelene radius (greatest distance from the center of the moon) varying between 9,300 km and 9,500 km and a periselene radius (shortest distance from the center of the moon) varying between 2,500 km and 2,700 km (reference 3). Both these satellites have a canted turnstile antenna located symmetrically with respect to the spin axis and both operate at VHF for purposes of obtaining range and range rate information.

The raw data received at the Goddard Range and Range Rate Tracking Stations from these satellites and analyzed in this report is the time T in seconds required to count a fixed number of cycles, N = 14,328, of the round-trip frequency shift f_d of the uplink carrier frequency* plus a known frequency offset, f_b = 30 KHz (reference 5). Since f_d is ordinarily much less than f_b, the time T is ordinarily about one half second. The data are collected at the rate of one measurement per second.

---

*The satellite transponder actually receives at one VHF frequency and transmits at another, making use of an onboard oscillator whose effect is removed on the ground in the processing of the received signal (reference 4). The overall effect of the signal processing, however, is to produce on the ground the same (except for the way that spin alters the measurement) result that would be obtained by coherently turning around in the ground transmitted carrier at the same frequency.

While the frequency offset f_b is constant, the frequency difference f_d, which is composed almost entirely of the two-way Doppler shift between the ground station and the satellite, may change somewhat over the half second counting interval. Since the frequency counted over this interval is the sum $f_d + f_b$, and since the average number of cycles per second is, of course, N/T, the average value of f_d is given by

$$f_d \doteq \bar{f}_d = (N/T) - f_b . \qquad (1)$$

Since $f_d << f_b$, using (1), T can be approximated by a linear function of f_d.

$$T \doteq (N/f_b) - (N/f_b^2)\, f_d . \qquad (2)$$

It is shown in Appendix A of this report that the phase pattern of the turnstile antenna can be expressed as a linear function plus a periodic function of the angle of rotation. As the satellite spins, the phase pattern introduces a bias in the two-way difference frequency f_d and hence T from equation (2). The bias results from the linear term in the phase pattern. Harmonics of the spin rate are caused by the periodic terms.

Since the data is sampled, the frequencies which appear are the beat frequencies between multiples of the sampling rate and harmonics of the spin rate f_s. Due to both geometrical and electrical symmetry of the antenna, the even harmonics of the spin rate predominate.

Although the sampling is not instantaneous, the periodicities still appear in the raw data. The counting of N cycles amounts to an integration of the instantaneous difference frequency, and if the latter is expanded in a Fourier series and integrated over the sampling period, term by term, the new series generated by this procedure contains exactly the same harmonic terms, although with different amplitudes and phases.

ANALYSIS

Figure 1 is a typical plot of the raw data analyzed in this report, i.e., the time in seconds T required to count a fixed number of cycles N (or zero crossings) of the two-way difference frequency f_d plus a reference frequency f_b. From inspection of the figure, it can be seen that there is a linear trend in the data.

The method of analysis used in this report (described in Appendix B) consisted in fitting a least squares straight line to the raw data, then determining the frequency content in the data by spectral analysis of the residuals from this straight line. Figure 2 is the spectral density of the residuals from a least squares straight line fitted to the raw data plotted in Figure 1.

It should be noted that a least squares straight line provides a better fit to the raw data analyzed in this report than a quadratic or higher order polynomial in the sense that the root mean square of the residuals is not improved by including higher order terms and that spectrum analysis of the residuals from a higher ordered polynomial (through 6th order) reveals the same periodicities.

It can be seen from inspection of Figure 2 that the following frequencies appear in the spectrum: 0.1730, 0.3080, 0.3460, 0.4135, and 0.4810 cycles/second.

From reference 6, the spin rate of Explorer 35 for 18 February 1968 was obtained as 24.81 rpm, or 0.4135 cycles/second. The peak in the spectrum at 0.4150 cycles/second, therefore, is the fundamental of the spin frequency. The appearance of the other frequencies in the data is due to the phenomenon of aliasing (Appendix B).

Since the sampling rate is 1/second, the maximum resolvable frequency is 0.5 cycles/second. Therefore, the frequencies 0.1730, 0.3080, 0.3460, and 0.4810 cycles/second which also appear in the spectrum are the beat frequencies between multiples of the sampling rate and harmonics of the spin rate f_s.

Twice the spin rate* beating with one multiple of the sampling rate is

$$1 - 2 f_s = 0.1730 \text{ cycles/second.} \qquad (3)$$

which corresponds with 0.1725 cycles/second.

---

*Here we are using for f_s the spin rate obtained from reference 6.

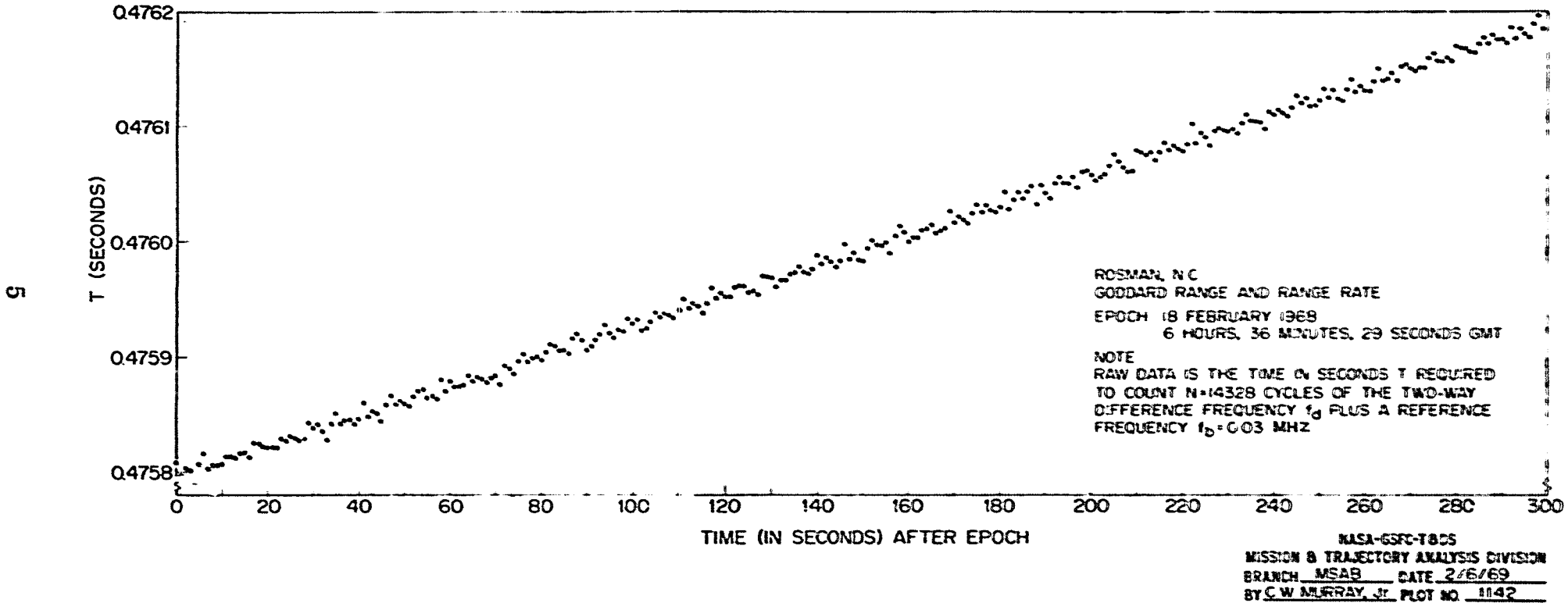

Figure 1–Explorer 35 Raw Data

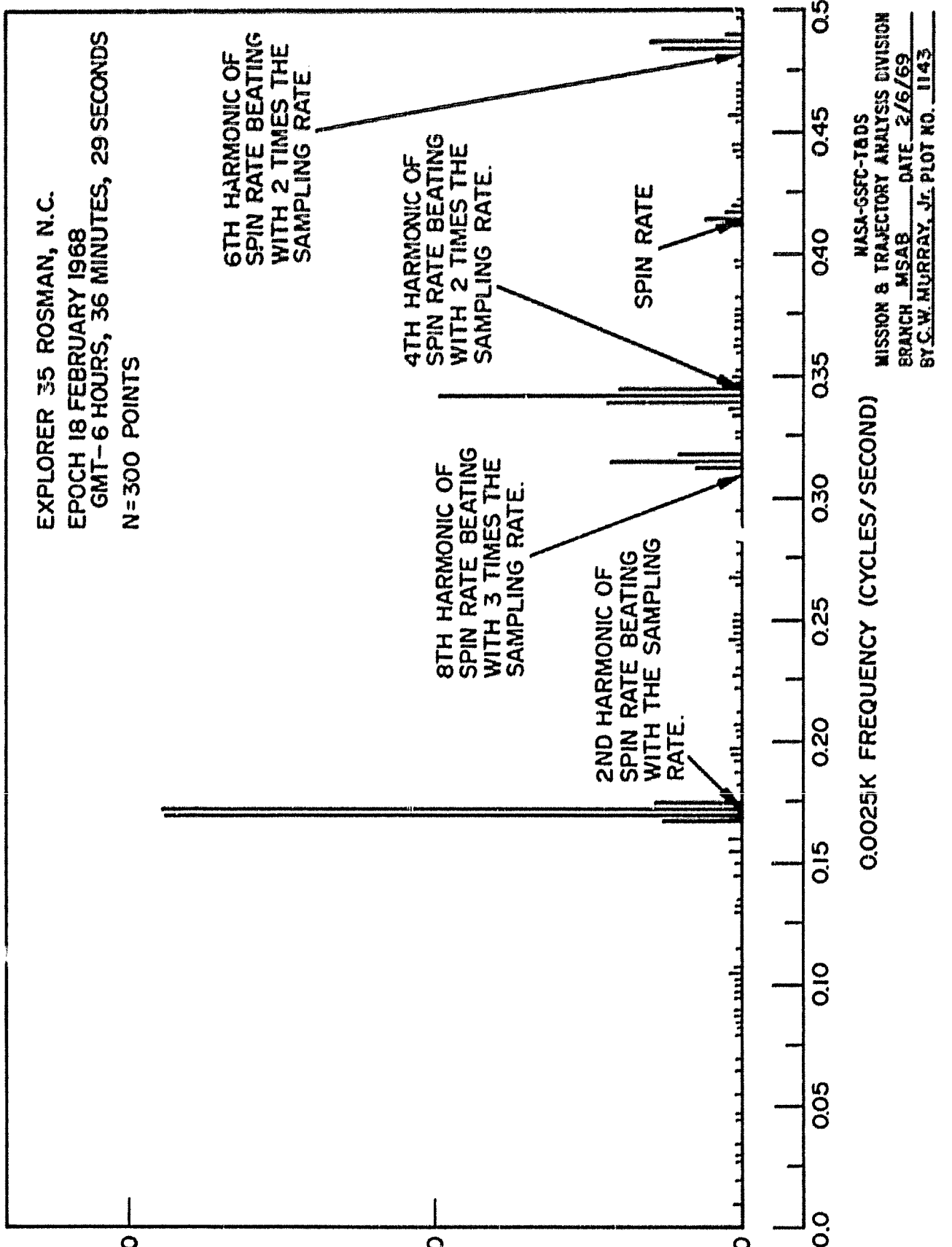

Figure 2–Spectral Density of Residuals from a Least Squares Straight Line Fitted to the Raw Data of Figure 1

Four times the spin rate beating with two multiples of the sampling rate is

$$2 - 4f_s = 0.3460 \text{ cycles/second,} \tag{4}$$

which corresponds with 0.3425 cycles/second.

Six times the spin rate beating with two multiples of the sampling rate is

$$6f_s - 2 = 0.4810 \text{ cycles/second,} \tag{5}$$

which corresponds with 0.4875 cycles/second.

Finally, eight times the spin rate beating with three multiples of the sampling rate is

$$8f_s - 3 = 0.3080 \text{ cycles/second,} \tag{6}$$

which corresponds with 0.3150 cycles/second.

Table I contains a Summary of the Data Analysis, giving satellite identification, epoch of the data (in Greenwich Mean Time), Goddard Range and Range Rate Tracking Station, number of points in the data stretch, spin rate and spin period of the satellite obtained from references 2, 3, 6, and 7, beat frequencies between multiples of the sampling rate and harmonics of the spin rate, and corresponding frequencies appearing in the spectrum of the residuals from a least squares straight line fitted to the data.

From inspection of Table I it can be seen that the even harmonics of the spin rate predominate. As shown in Appendix A, this is due to both geometrical and electrical symmetry of the antenna configuration used on Explorers 33 and 35.

APPLICATION OF A NON-LINEAR MODEL TO THE DATA

Having determined through spectral analysis which beat frequencies predominate, this information can be used to construct a more accurate model for the data. By applying a nonlinear regression technique (reference 8), least squares estimates for the parameters of the model can then be obtained. There are two results:

Table I
Data Analysis Summary

Explorer	Epoch (GMT)	Station	Number of Points	Spin Period T_s (seconds) / Spin Rate f_s* (cycles/sec)	Harmonics of the spin rate f_s beating with multiples of the sampling frequency of 1 sample/sec. (cycles/sec)	Frequencies appearing in power spectral density of residuals from best fitted straight line. First frequency is larger in amplitude. (cycles/sec)
33	2 July 1966 6h-21m-5s	Rosman	276	2.30 sec 0.4348 Hz	$1-2f_s$ = 0.1304 $2-4f_s$ = 0.2608 $3-6f_s$ = 0.3912	0.12 and 0.14 0.24 and 0.26 0.38 and 0.36
33	2 July 1966 10h-1m-5s	Santiago	288	2.30 sec 0.4348 Hz	$1-2f_s$ = 0.1304 $2-4f_s$ = 0.2608 $3-6f_s$ = 0.3912	0.12 and 0.14 0.24 and 0.26 0.38 and 0.36
33	2 July 1966 11h-1m-29s	Santiago	256	2.30 sec 0.4348 Hz	$1-2f_s$ = 0.1304 $2-4f_s$ = 0.2608 $3-6f_s$ = 0.3912	0.12 and 0.14 0.26 and 0.24 0.38 and 0.36
33	2 July 1966 19h-21m-59s	Carnarvon	160	2.30 sec 0.4348 Hz	$1-2f_s$ = 0.1304 $2-4f_s$ = 0.2608 $3-6f_s$ = 0.3912	0.12 and 0.14 Not observed. Not observed.
33	2 July 1966 20h-23m-3s	Carnarvon	224	2.30 sec 0.4348 Hz	$1-2f_s$ = 0.1304 $2-4f_s$ = 0.2608 $3-6f_s$ = 0.3912	0.12 and 0.14 Not observed. 0.38 and 0.36
33	3 July 1966 15h-11m-57s	Carnarvon	256	2.30 sec 0.4348 Hz	$1-2f_s$ = 0.1304 $2-4f_s$ = 0.2608 $3-6f_s$ = 0.3912	0.12 and 0.14 0.26 and 0.24 Not observed.

Table I–(Continued)

Explorer	Epoch (GMT)	Station	Number of Points	Spin Period T_s (seconds) / Spin Rate f_s* (cycles/sec)	Harmonics of the spin rate f_s beating with multiples of the sampling frequency of 1 sample/sec. (cycles/sec)	Frequencies appearing in power spectral density of residuals from best fitted straight line. First frequency is larger in amplitude. (cycles/sec)
33	7 July 1966 4h-2m-51s	Santiago	256	2.29 sec 0.4367 Hz	1-2f_s 0.1266 2-4f_s 0.2532 3-6f_s 0.3798	0.12 and 0.14 0.24 and 0.26 0.36 and 0.38
33	7 July 1966 16h-34m-22s	Carnarvon	320	2.29 sec 0.4367 Hz	1-2f_s 0.1266 2-4f_s 0.2532 3-6f_s 0.3798	0.12 and 0.14 0.30 and 0.32 Not observed.
33	8 July 1966 2h-6m-1s	Madagascar	192	2.29 sec 0.4367 Hz	1-2f_s 0.1266 2-4f_s 0.2532 3-6f_s 0.3798	Not observed. 0.24 and 0.26 Not observed.
33	8 July 1966 8h-31m-54s	Rosman	288	2.29 sec 0.4367 Hz	1-2f_s 0.1266 2-4f_s 0.2532 3-6f_s 0.3798	0.12 and 0.14 0.24 and 0.26 0.36 and 0.38
33	18 Jan 1967 8h-21m-48s	Carnarvon	252	3.33 sec 0.3003 Hz	1-2f_s 0.3994	0.3875 and 0.3900
33	22 Jan 1967 17h-0m-28s	Rosman	276	3.33 sec 0.3003 Hz	f_s 0.3003 1-2f_s 0.3994 4f_s - 1 0.2012	0.3025 and 0.3050 0.3925 and 0.3950 0.2125 and 0.2150
33	24 Jan 1967	Rosman	220	3.33 0.3003	f_s 0.3003 1-2f_s 0.3994 4f_s-1 0.2012	0.300 and 0.305 0.395 and 0.400 0.205 and 0.210
33	25 Jan 1967	Carnarvon	60	3.33 0.3003	1-2f_s 0.3994 4f_s-1 0.2012	0.400 and 0.375 0.225 and 0.200
33	25 Jan 1967 4h-52m-52s	Carnarvon	64	3.33 sec 0.3003 Hz	1-2f_s 0.3994 4f_s - 1 0.2012	0.400 and 0.375 0.200 and 0.225

Table I–(Continued)

Explorer	Epoch (GMT)	Station	Number of Points	Spin Period T_s (seconds) Spin Rate f_s* (cycles/sec)	Harmonics of the spin rate f_s beating with multiples of the sampling frequency of 1 sample/sec. (cycles/sec)	Frequencies appearing in power spectral density of residuals from best fitted straight line. First frequency is larger in amplitude. (cycles/sec)
33	25 Jan 1967 17h-32m-38s	Rosman	200	3.33 sec 0.3003 Hz	$1-2f_s = 0.3994$ $4f_s - 1 = 0.2012$	0.395 and 0.400 0.210 and 0.205
33	12 Aug 1967 8h-13m-14s	Santiago	232	2.32 sec 0.4310 Hz	$1-2f_s = 0.1380$ $2-4f_s = 0.2760$ $3-6f_s = 0.4140$	0.14 and 0.12 0.28 and 0.30 0.42 and 0.44
33	14 Aug 1967 9h-11m-22s	Carnarvon	192	2.32 sec 0.4310 Hz	$1-2f_s = 0.1380$ $2-4f_s = 0.2760$ $3-6f_s = 0.4140$	0.14 and 0.12 0.28 and 0.30 0.42
33	14 Aug 1967 20h-41m-6s	Madagascar	224	2.32 sec 0.4310 Hz	$1-2f_s = 0.1380$ $2-4f_s = 0.2760$ $3-6f_s = 0.4140$	0.14 and 0.12 Not observed. 0.44 and 0.42
33	17 Aug 1967 11h-25m-2s	Carnarvon	224	2.32 sec 0.4310 Hz	$1-2f_s = 0.1380$ $2-4f_s = 0.2760$ $3-6f_s = 0.4140$	0.14 and 0.12 0.28 and 0.30 0.42 and 0.44
35	19 Jul 1967 17h-6m-44s	Carnarvon	160	2.14 sec 0.4673 Hz	$1-2f_s = 0.0654$	0.06 and 0.07
35	23 Jul 1967 13h-46m-17s	Carnarvon	160	2.17 sec 0.4608 Hz	$1-2f_s = 0.0784$	0.08 and 0.07
35	23 July 1967 17h-33m-16s	Carnarvon	160	2.17 sec 0.4608 Hz	$1-2f_s = 0.0784$	0.08 and 0.07

Table I–(Continued)

Explorer	Epoch (GMT)	Station	Number of Points	Spin Period T_s (seconds) / Spin Rate f_s* (cycles/sec)	Harmonics of the spin rate f_s beating with multiples of the sampling frequency of 1 sample/sec. (cycles/sec)	Frequencies appearing in power spectral density of residuals from best fitted straight line. First frequency is larger in amplitude. (cycles/sec)
35	18 Feb 1968 6h-36m-29s	Rosman	300	2.42 sec 0.4135 Hz	f_s = 0.4135 $1-2f_s$ = 0.1730 $2-4f_s$ = 0.3460 $6f_s-2$ = 0.4810 $8f_s-3$ = 0.3080	0.4150 and 0.4125 0.1725 and 0.1700 0.3425 and 0.3400 0.4875 and 0.4850 0.3150 and 0.3175
35	19 Feb. 1968 5h-42m-14s	Madagascar	96	2.42 sec 0.4135 Hz	$1-2f_s$ = 0.1730 $2-4f_s$ = 0.3460 $6f_s-2$ = 0.4810 $8f_s-3$ = 0.3080	0.1722 and 0.1667 0.3444 and 0.3389 0.4889 and 0.4833 0.3111 and 0.3056
35	19 Feb 1968 13h-23m-19s	Santiago	84	2.42 sec 0.4135 Hz	$1-2f_s$ = 0.1730 $2-4f_s$ = 0.3460 $6f_s-2$ = 0.4810 $8f_s-3$ = 0.3080	0.17 and 0.18 0.34 and 0.35 0.49 and 0.48 0.31 and 0.32
35	20 Feb 1968 17h-17m-34s	Carnarvon	300	2.42 sec 0.4135 Hz	$1-2f_s$ = 0.1730 $2-4f_s$ = 0.3460 $6f_s-2$ = 0.4810 $8f_s-3$ = 0.3080	0.1725 and 0.1700 0.3425 and 0.3450 0.4850 and 0.4875 0.3150 and 0.3125
35	20 Aug 1968 16h-9m-46s	Rosman	88	2.41 sec 0.4140 Hz	$1-2f_s$ = 0.1720 $2-4f_s$ = 0.3440 $6f_s-2$ = 0.4840 $8f_s-3$ = 0.3120	0.17 and 0.18 0.34 and 0.33 0.49 and 0.48 0.32 and 0.33

Table I–(Continued)

Explorer	Epoch (GMT)	Station	Number of Points	Spin Period T_s (seconds) / Spin Rate f_s* (cycles/sec)	Harmonics of the spin rate f_s beating with multiples of the sampling frequency of 1 sample/sec. (cycles/sec)	Frequencies appearing in power spectral density of residuals from best fitted straight line. First frequency is larger in amplitude. (cycles/sec)
35	21 Aug 1968 1h-33m-43s	Carnarvon	280	2.41 sec 0.4140 Hz	f_s = 0.4140 $1-2f_s$ = 0.1720 $2-4f_s$ = 0.3440 $6f_s-2$ = 0.4840 $8f_s-3$ = 0.3120	0.4150 and 0.4125 0.1700 and 0.1725 0.3400 and 0.3425 0.4875 and 0.4900 0.3175 and 0.3200
35	24 Aug 1968 15h-51m-13s	Santiago	196	2.41 sec 0.4140 Hz	f_s = 0.4140 $1-2f_s$ = 0.1720 $2-4f_s$ = 0.3440 $6f_s-2$ 0.4840 $8f_s-3$ 0.3120	0.4150 and 0.4100 0.1700 and 0.1750 0.3400 and 0.3450 0.4950 and 0.5000 0.3200 and 0.3150
35	24 Aug 1968 23h-17m-55s	Alaska	144	2.41 sec 0.4140 Hz	$1-2f_s$ = 0.1720 $2-4f_s$ 0.3440 $6f_s-2$ 0.4840 $8f_s-3$ 0.3120	0.1700 and 0.1750 0.3450 and 0.3400 0.4900 and 0.4950 Not observed.

*References 2, 3, 6, and 7.

1. The spin rate of the satellite can be determined from the data in a least squares sense.

2. The rms of the residuals from this non-linear model will be reduced over that of a straight line.

In order to demonstrate the above, the following non-linear model was applied to raw data taken at Rosman, N.C., on 18 February 1968, 6 hours, 36 minutes, 29 seconds GMT, and at Carnarvon, Australia, on 20 February 1968, 17 hours, 17 minutes, 34 seconds, GMT, from Explorer 35 (AIMP-E).

$$T_i = c_1 + c_2 i + a_1 \sin(2\pi f_s i) + b_1 \cos(2\pi f_s i) + a_2 \sin(2\pi(1 - 2f_s)i)$$

$$+ b_2 \cos(2\pi(1 - 2f_s)i) + a_3 \sin(2\pi(2 - 4f_s)i) + b_3 \cos(2\pi(2 - 4f_s)i)$$

$$+ a_4 \sin(2\pi(6f_s - 2)i) + b_4 \cos(2\pi(6f_s - 2)i) + a_5 \sin(2\pi(8f_s - 3)i) \qquad (7)$$

$$+ b_5 \cos(2\pi(8f_s - 3)i)$$

$$(i = 1, 2, \cdots, 300)$$

where c_1, c_2, a_1, a_2, a_3, a_4, a_5, b_1, b_2, b_3, b_4, b_5, f_s are the parameters of the model.

For each data stretch 300 points were available. A generalized least squares program (reference 8) was used to find the best estimates of the parameters in the above model. That is, the parameters were solved for in the program to minimize the sum of the squares of the residuals of the data points from the model. Results of the analysis can be seen in Table II which shows the solution for each parameter with its associated uncertainty or standard deviation. (See Appendix C for the standard deviation of a least squares estimate in a non-linear regression model.)

From Table II the solution for the spin rate of Explorer 35 on 18 February 1968 using the Rosman data is $\hat{f}_s$ = 0.41440654 cycles/second (24.8644 rpm) with

Table II
Comparison of Non-Linear Model With Straight Line
Fitted to Explorer 35 Data
(Least Squares)

Station: Rosman, N.C.
Epoch: 18 February 1968, 6 hours, 36 minutes, 29 seconds GMT.
Number of Points: 300
Straight Line Model:

$$T_i = a_0 + a_1 i \qquad (i = 1, 2, 3, \ldots, 300)$$

Estimate of Parameter:	Standard Deviation of Parameter Estimate
$\hat{a}_0$ 0.47579445 sec	$\sigma_{\hat{a}_0}$ $(0.57549889)\ 10^{-6}$ sec
$\hat{a}_1$ $(0.13103713)\ 10^{-5}$ (dimensionless)	$\sigma_{\hat{a}_1}$ $(0.33143597)\ 10^{-8}$ (dimensionless)

RMS of residuals = $0.49715118 \times 10^{-5}$ seconds (32 cm/second)

Non-Linear Model:

$$T_i = c_1 + c_2 i + a_1 \sin(2\pi f_s i) + b_1 \cos(2\pi f_s i) + a_2 \sin(2\pi(1 - 2f_s)i)$$
$$+ b_2 \cos(2\pi(1 - 2f_s)i) + a_3 \sin(2\pi(2 - 4f_s)i)$$
$$+ b_3 \cos(2\pi(2 - 4f_s)i) + a_4 \sin(2\pi(6f_s - 2)i)$$
$$+ b_4 \cos(2\pi(6f_s - 2)i) + a_5 \sin(2\pi(8f_s - 3)i)$$
$$+ b_5 \cos(2\pi(8f_s - 3)i) \qquad (i = 1, 2, 3, \ldots, 300)$$

Table II–(Continued)

Estimate of Parameter:		Standard Deviation of Parameter Estimate	
$\hat{c}_1$	0.47579569 sec	$\sigma_{\hat{c}_1}$	$(0.27217461)\ 10^{-6}$ sec
$\hat{c}_2$	$(0.13106123)\ 10^{-5}$ (dimensionless)	$\sigma_{\hat{c}_2}$	$(0.15753571)\ 10^{-8}$ (dimensionless)
$\hat{a}_1$	$(0.68193717)\ 10^{-6}$ sec	$\sigma_{\hat{a}_1}$	$(0.19377216)\ 10^{-6}$ sec
$\hat{f}_s$	0.41440654 (cycles/sec)	$\sigma_{\hat{f}_s}$	$(0.1503465?)\ 10^{-4}$ (cycles/sec)
$\hat{b}_1$	$(0.81426620)\ 10^{-6}$ sec	$\sigma_{\hat{b}_1}$	$(0.19271141)\ 10^{-6}$ sec
$\hat{a}_2$	$(0.20113182)\ 10^{-5}$ sec	$\sigma_{\hat{a}_2}$	$(0.22455975)\ 10^{-6}$ sec
$\hat{b}_2$	$(0.40956804)\ 10^{-5}$ sec	$\sigma_{\hat{b}_2}$	$(0.20092015)\ 10^{-6}$ sec
$\hat{a}_3$	$-(0.16844185)\ 10^{-5}$ sec	$\sigma_{\hat{a}_3}$	$(0.24293704)\ 10^{-6}$ sec
$\hat{b}_3$	$(0.25006524)\ 10^{-5}$ sec	$\sigma_{\hat{b}_3}$	$(0.21283401)\ 10^{-6}$ sec
$\hat{a}_4$	$(0.12792709)\ 10^{-5}$ sec	$\sigma_{\hat{a}_4}$	$(0.21874661)\ 10^{-6}$ sec
$\hat{b}_4$	$(0.12415350)\ 10^{-5}$ sec	$\sigma_{\hat{b}_4}$	$(0.21941388)\ 10^{-6}$ sec
$\hat{a}_5$	$-(0.15831928)\ 10^{-5}$ sec	$\sigma_{\hat{a}_5}$	$(0.22593718)\ 10^{-6}$ sec
$\hat{b}_5$	$(0.10895869)\ 10^{-5}$ sec	$\sigma_{\hat{b}_5}$	$(0.26449528)\ 10^{-6}$ sec

RMS of residuals = $(0.23628070)\ 10^{-5}$ seconds (15 cm/sec).

Station: Carnarvon, Australia

Epoch: 20 February 1968, 17 hours, 17 minutes, 34 seconds GMT.

Number of Points: 300

Straight Line Model:

$$T_i = a_0 + a_1 i$$

$$(i = 1, 2, \ldots, 300)$$

Table II–(Continued)

Estimate of Parameter:		Standard Deviation of Parameter Estimate	
$\hat{a}_0$	0.48093082 sec	$\sigma_{\hat{a}_0}$	$(0.77376408)\ 10^{-6}$ sec
$\hat{a}_1$	$(0.90051096)\ 10^{-6}$ (dimensionless)	$\sigma_{\hat{a}_1}$	$(0.44561901)\ 10^{-8}$ (dimensionless)

RMS of Residuals = $(0.66842480)\ 10^{-5}$ seconds (42 cm/sec)

Non-Linear Model:

$$T_i = c_1 + c_2 i + a_1 \sin(2\pi f_s i) + b_1 \cos(2\pi f_s i) + a_2 \sin(2\pi(1 - 2f_s)i)$$

$$+ b_2 \cos(2\pi(1 - 2f_s)i) + a_3 \sin(2\pi(2 - 4f_s)i) + b_3 \cos(2\pi(2 - 4f_s)i)$$

$$+ a_4 \sin(2\pi(6f_s - 2)i) + b_4 \cos(2\pi(6f_s - 2)i) + a_5 \sin(2\pi(8f_s - 3)i)$$

$$+ b_5 \cos(2\pi(8f_s - 3)i)$$

$$(i = 1, 2, 3, \ldots, 300)$$

Estimate of Parameter:		Standard Deviation of Parameter Estimate	
$\hat{c}_1$	(0.48093177) sec	$\sigma_{\hat{c}_1}$	$(0.23114225)\ 10^{-6}$ sec
$\hat{c}_2$	$(0.90050782)\ 10^{-6}$ (dimensionless)	$\sigma_{\hat{c}_2}$	$(0.13378799)\ 10^{-8}$ (dimensionless)
$\hat{a}_1$	$-(0.61840445)\ 10^{-6}$ sec	$\sigma_{\hat{a}_1}$	$(0.16438325)\ 10^{-6}$ sec
$\hat{f}_s$	(0.41435270) cycles/sec	$\sigma_{\hat{f}_s}$	$(0.98549050)\ 10^{-5}$ (cycles/sec)
$\hat{b}_1$	$-(0.54222824)\ 10^{-6}$ sec	$\sigma_{\hat{b}_1}$	$(0.16351419)\ 10^{-6}$ sec
$\hat{a}_2$	$-(0.60332663)\ 10^{-5}$ sec	$\sigma_{\hat{a}_2}$	$(0.17983013)\ 10^{-6}$ sec
$\hat{b}_2$	$-(0.40009164)\ 10^{-5}$ sec	$\sigma_{\hat{b}_2}$	$(0.19779028)\ 10^{-6}$ sec
$\hat{a}_3$	$(0.47320679)\ 10^{-6}$ sec	$\sigma_{\hat{a}_3}$	$(0.22675795)\ 10^{-6}$ sec

Table II–(Continued)

Estimate of Parameter:	Standard Deviation of Parameter Estimate
$\hat{b}_3$ (0.41969521) 10^{-5} sec	$\sigma_{\hat{b}_3}$ (0.16472243) 10^{-6} sec
$\hat{a}_4$ -(0.10093327) 10^{-5} sec	$\sigma_{\hat{a}_4}$ (0.21249993) 10^{-6} sec
$\hat{b}_4$ -(0.24523666) 10^{-5} sec	$\sigma_{\hat{b}_4}$ (0.17110756) 10^{-6} sec
$\hat{a}_5$ -(0.13510547) 10^{-5} sec	$\sigma_{\hat{a}_5}$ (0.18353051) 10^{-6} sec
$\hat{b}_5$ -(0.10807196) 10^{-5} sec	$\sigma_{\hat{b}_5}$ (0.19343074) 10^{-6} sec
RMS of Residuals = (0.20065898) 10^{-5} seconds (13 cm/sec)	

an uncertainty of 0.1503×10^{-4} cycles/second (0.0009 rpm). The solution for the spin rate of Explorer 35 on 20 February 1968 using the Carnarvon data is f_s = 0.41435270 cycles/second (24.8612 rpm) with an uncertainty of 0.0985×10^{-4} cycles/second (0.0006 rpm).

Also, the rms of the residuals from the model using the Rosman data is $0.23628070 \times 10^{-5}$ seconds (or 15 cm/sec) while the rms of the residuals from a straight line fitted to the same data is $0.49715118 \times 10^{-5}$ seconds (or 32 cm/sec). The rms of the residuals from the model using the Carnarvon data is $0.20065898 \times 10^{-5}$ seconds (or 13 cm/sec), while the rms of the residuals from a straight line fitted to the same data is $0.66842480 \times 10^{-5}$ seconds (or 42 cm/sec).

Application of a slightly different model to account for only the second and fourth harmonics of the spin rate had little effect on the least squares solution for the spin rate. However, the rms of the residuals from this latter model was higher than the rms of the residuals from the model in (7).

CONCLUSIONS

Results of a spectrum analysis of the residuals from a least squares straight line fitted to two-way Doppler data (the time in seconds required to count a fixed number of cycles of the two-way difference frequency plus a reference frequency) received at Goddard Range and Range Rate Tracking Stations from the Explorer 33 (AIMP-D) and Explorer 35 (AIMP-E) satellites reveal that:

1. The spin rate and harmonics of the spin rate can be detected in the data.

Using a simple model for the VHF turnstile antenna configuration on these satellites, it is shown that tl ₃ antenna phase pattern can be expressed as a linear function plus a periodic function of the angle of rotation. As the satellite spins, the varying phase pattern introduces a bias in the two-way difference frequency. Results of the antenna analysis indicate that:

2. A bias of several centimeters per second in the two-way Doppler data results from the linear term in the antenna phase pattern.

3. Harmonics of the spin rate are caused by the periodic terms in the antenna phase pattern.

Applying a non-linear model to the raw data, the spin rate of the satellite can be determined in a least squares sense. For the two examples given in the report, the rms of the residuals from the non-linear model was reduced by a factor of 1/2 and 1/3 compared to the rms of the residuals from a least squares straight line fitted to the same data – from 32 cm/sec to 15 cm/sec and from 42 cm/sec to 13 cm/sec.

ACKNOWLEDGEMENT

The authors wish to express their gratitude to Mr. Lowell Elfenbein (formerly with the Mission and Systems Analysis Branch) for the computer program which calculated the spectral density of the residuals.

REFERENCES

1. "AIMP (IMP-D) Technical Summary Description," X-724-67-87, NASA, GSFC, March 1967.

2. Madden, J. J., "Second Interim Flight Report, AIMP-I, Explorer 33," X-724-67-223, NASA, GSFC, May 1967.

3. Madden, J. J., and Brahm, J. J., "Explorer 35 First Interim Report And Explorer 33 Third Interim Report And The AIMP Project Bibliography," X-724-68-45, NASA, GSFC, March 1968.

4. Kronmiller, G., Jr. and Baghdady, E., "The Goddard Range and Range Rate Tracking System: Concept, Design, and Performance," GSFC Report X-531-65-403, October 1965.

5. "Design Evaluation Report, Goddard Range and Range Rate System," General Dynamics Report R-67-042, 13 Dec. 1967. Contract NAS 5-10555.

6. Madden, J. J., Private Communication.

7. Madden, J. J., "Interim Flight Report, Anchored Interplanetary Monitoring Platform, AIMP I-Explorer 33," X-724-66-588, NASA, GSFC, December 1966.

8. A General Weighted Least-Squares-Fit Subroutine, Goddard Program No. D00107, T. A. Orlow, NOL TN 7578.

9. Jackson, R. B., "The Canted Turnstile as an Omnidirectional Spacecraft Antenna System," GSFC Report X-712-67-441, Sept. 1967.

10. Ramo, S. and Whinnery, J., "Fields and Waves in Modern Radio," John Wiley & Sons, N.Y.; 1959. Paragraphs 12.06 and 12.09.

11. Bolljahn, J., "Effects of Satellite Spin on Ground-Received Signal," IRE Trans. on Antennas and Propagation, July 1958; pp. 260-267.

12. Blackman, R. B., and Tukey, J. W., "The Measurement of Power Spectra," New York: Dover Publications, Inc., 1959.

13. Anderson, J. D., "Determination of the Masses of the Moon and Venus and the Astronomical Unit from Radio Tracking Data of the Mariner II Spacecraft," NASA, Jet Propulsion Laboratory, TR 32-816 (July 1, 1967).

14. Kendall, M. G., and Stuart, A., "The Advanced Theory of Statistics," Vol. 2, Hafner Publishing Company, N. Y. (1967), pp. 76 and 82.

APPENDIX A

Periodic Properties of a Rotating Turnstile Antenna

Both Explorer 33 and Explorer 35 satellites make use of a canted turnstile antenna (Reference 9) consisting of four quarter-wave monopoles spaced symmetrically about the spin axis of the satellite as shown in Figure A1. The monopoles are fed with relative phase angles of 0°, 90°, 180° and 270° so that opposing terminals are 180° out of phase. The exact radiation pattern of such an antenna would be difficult to calculate in view of the irregular shape of the body of the satellite and the presence of the booms and the solar paddles. Some general properties of the radiation pattern, nevertheless, can be derived by examining a simple model of the antenna system.

The model adapted for this purpose is a pair of crossed center-fed dipoles, driven in phase quadrature. Such an arrangement preserves the phase relationships used in the satellite antennas, since a center-fed dipole is equivalent to two opposing monopoles fed 180° out of phase. The dipoles will be assumed to be no longer than a half wave in length.

The model is illustrated in Figure A-2. The dipoles, each of length 2ℓ, lie in the x-y plane.

The currents on the dipoles, $I_1(x)$ and $I_2(y)$, are assumed to be standing waves. They can be written as

$$I_1(x) = I_1\ [I_1(x)/I_1] \equiv I_1 f(x)$$

$$I_2(y) = I_2\ [I_2(x)/I_2] \equiv I_2 f(y) \qquad \text{(A1)}$$

where the normalized functions f (x) and f (y) describing the shape of the currents on the dipoles have identical forms since the dipoles are assumed to have equal lengths. I_1 and I_2 are defined to be the currents at the center of the first and second dipoles respectively so that

$$f(0) = 1$$

$$f(\ell) = 0. \qquad \text{(A2)}$$

Because of the geometrical symmetry it will also be true that f is an even function

$$f(x) = f(-x). \tag{A3}$$

The customary assumption that $f(x)$ has a sinusoidal form is not needed in the analysis that follows.

The usual spherical polar coordinates r , θ and ϕ are used to describe the electric intensity of the radiation field of the antenna system. This electric intensity will have the components $E_\theta\,(r,\theta,\phi)$ and $E_\phi\,(r,\theta,\phi)$ only, since $E_r\,(r,\theta,\phi)$ is negligible in the far field.

The field components are easily derived using standard procedures (Reference 10). The components are

$$E_\theta = -j\eta k\,\frac{e^{-jkr}}{2\pi r}\cos\theta\left[I_2\sin\phi\int_0^\ell f(y)\cos(ky\sin\theta\sin\phi)\,dy + I_1\cos\phi\int_0^\ell f(x)\cos(kx\sin\theta\cos\phi)\,dx\right] \tag{A4}$$

$$E_\phi = -j\eta k\,\frac{e^{-jkr}}{2\pi r}\left[+I_2\cos\phi\int_0^\ell f(y)\cos(ky\sin\theta\sin\phi)\,dy - I_1\sin\phi\int_0^\ell f(x)\cos(kx\sin\theta\cos\phi)\,dx\right] \tag{A5}$$

in which use has been made of (A3). Here η is the characteristic impedence of free space and k is the wave number $k = 2\pi/\lambda$ where λ is the wavelength of the emitted radiation. The factor exp $j\omega t$ is understood.

Assume that the current at the terminals of the second antenna leads that at the terminals of the first antenna by 90° so that the antennas are fed in quadrature; and assume also that the magnitude of the feed currents are equal. Then

$$I_2 = j\,I_1\,. \tag{A6}$$

REPRODUCED FROM
REFERENCE 9

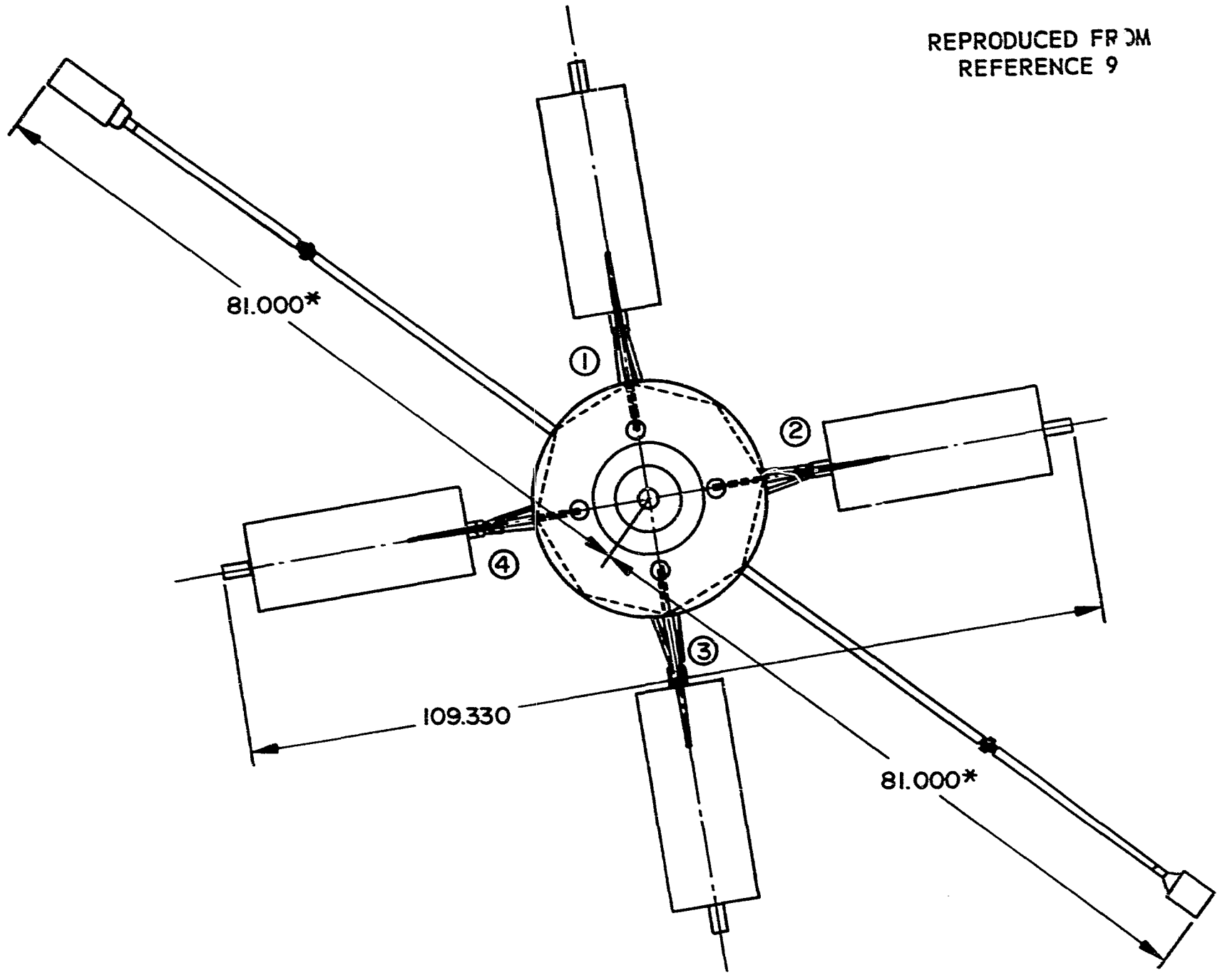

Figure A1–Explorer 35 Satellite

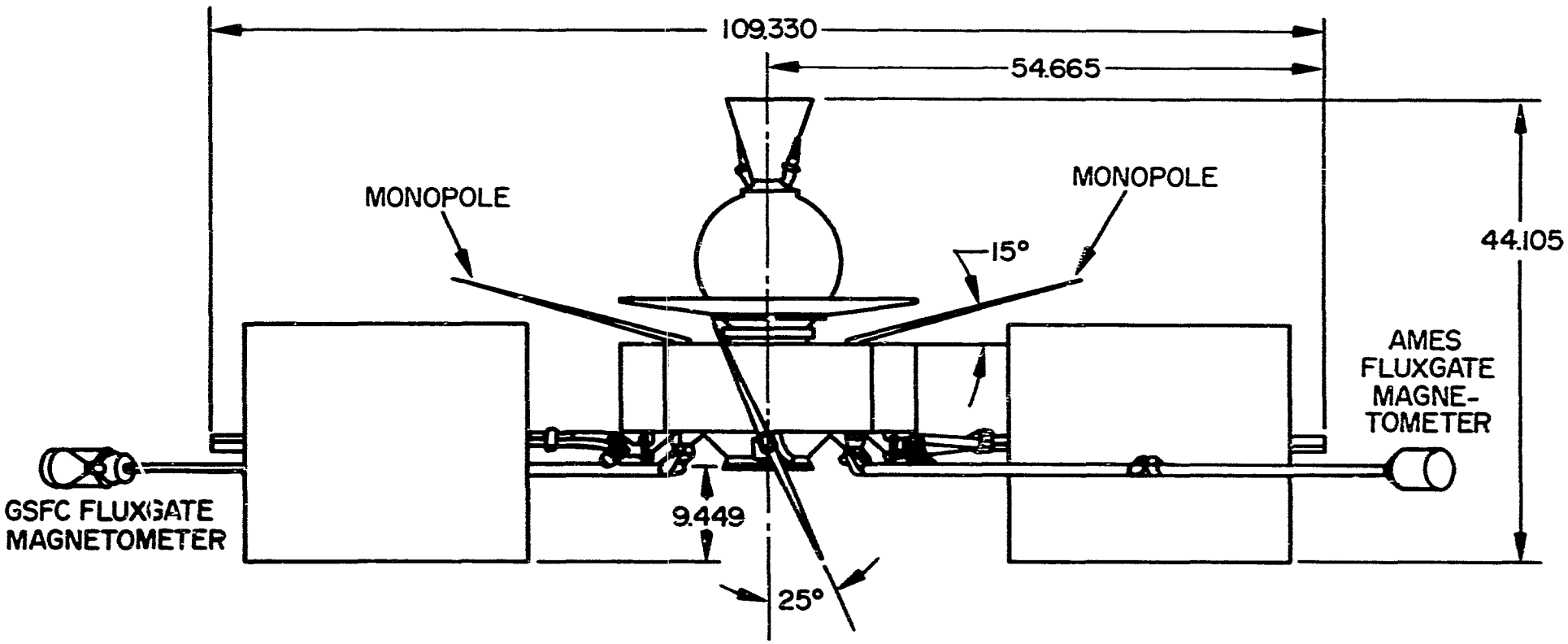

Figure A1(Continued)–Explorer 35 Satellite

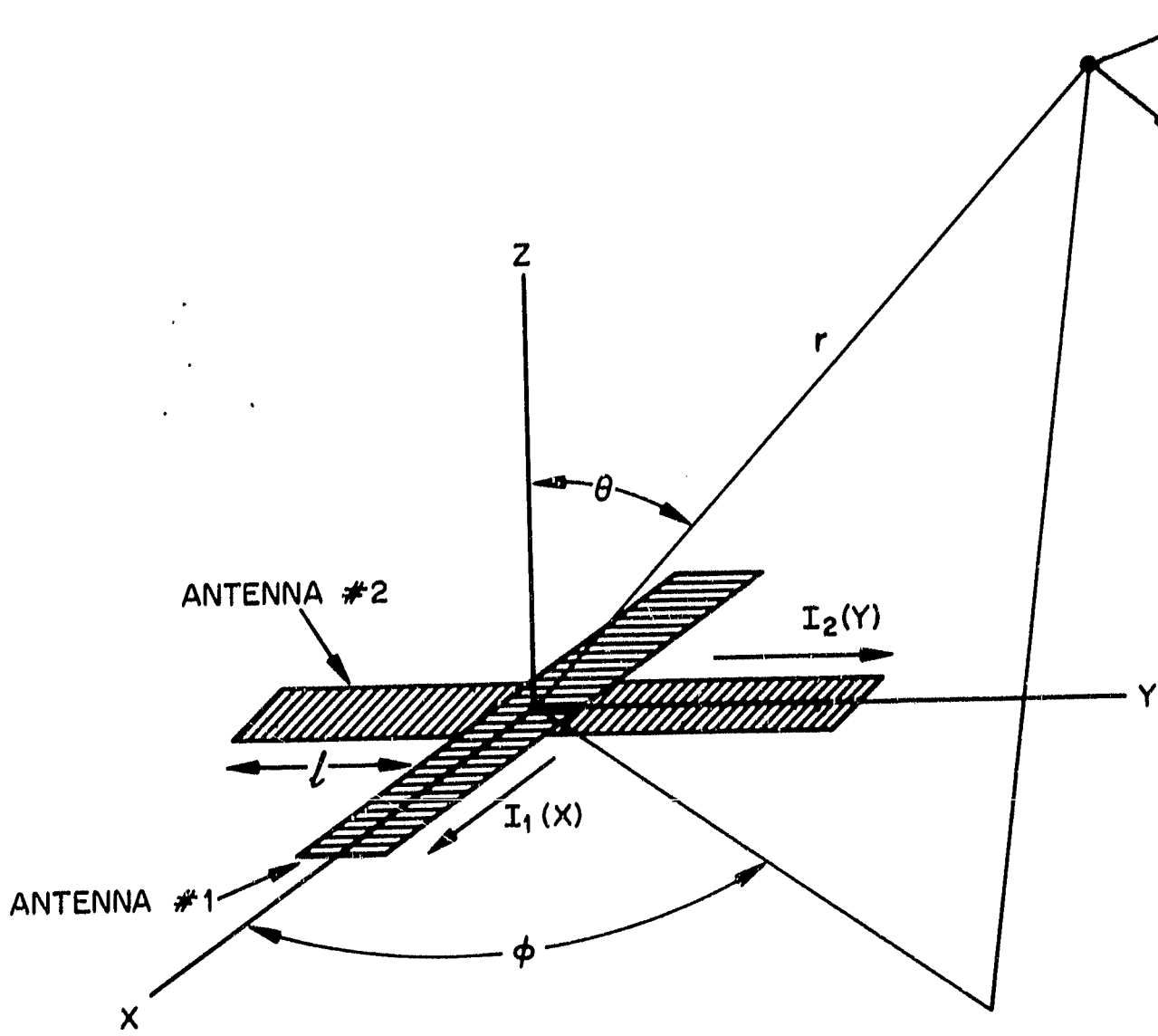

NASA-GSFC-T&DS
MISSION & TRAJECTORY ANALYSIS DIVISION
BRANCH MSAB DATE 2/6/69
BY J.W.MARINI PLOT NO. 1144

Figure A2–Crossed Dipole Antenna System

Equations A4 and A5 become

$$E_\theta = I_1 \eta k \frac{e^{-jkr}}{2\pi r} \cos\theta \left[\sin\phi \int_0^\ell f(y) \cos(ky \sin\theta \sin\phi)\, dy - j \cos\phi \int_0^\ell f(x) \cos(kx \sin\theta \cos\phi)\, dx \right] \tag{A7}$$

$$E_\phi = I_1 \eta k \frac{e^{-jkr}}{2\pi r} \left[\cos\phi \int_0^\ell f(y) \cos(ky \sin\theta \sin\phi)\, dy + j \sin\phi \int_0^\ell f(x) \cos(kx \sin\theta \cos\phi)\, dx \right]. \tag{A8}$$

The purpose of this analysis is to examine the behavior of the phase pattern of the antenna as a function of the angle ϕ, since, as the antenna spins, the field point relative to the antenna has fixed values of r and θ, but a varying value of ϕ. By direct substitution into equations (A7) and (A8) it can be seen that

$$E_\theta \left(\phi + \frac{\pi}{2}\right) = j\, E_\theta(\phi) = E_\theta(\phi)\, e^{j\pi/2} \tag{A9}$$

$$E_\phi \left(\phi + \frac{\pi}{2}\right) = j\, E_\phi(\phi) = E_\phi(\phi)\, e^{j\pi/2}. \tag{A10}$$

Fixing attention on E_ϕ (similar arguments apply to the E_θ component), and writing this component in polar form

$$E_\phi \equiv A(\phi)\, e^{j\,\alpha(\phi)}. \tag{A11}$$

Equation (A10) requires that

$$\begin{aligned} A\left(\phi + \frac{\pi}{2}\right) &= A(\phi) \\ \alpha\left(\phi + \frac{\pi}{2}\right) &= \alpha(\phi) + \frac{\pi}{2} + 2\pi n \end{aligned} \tag{A12}$$

where n is an integer. In the case under consideration, where the dipoles are a half wave length or less, n must be equal to zero. This follows because both of the integrals appearing in (A8) are positive for all values of ϕ since none of the factors in the integrands goes negative over the range of integration. A non-zero value for n would require that the complex number in the brackets in (A8) must circle the origin as ϕ is increased by $\pi/2$, but this is impossible since cos ϕ + j sin ϕ does not circle the origin over this increment.

Consequently

$$\alpha\left(\phi + \frac{\pi}{2}\right) = \alpha(\phi) + \frac{\pi}{2} \tag{A14}$$

whence $\alpha(\phi) - \phi$ is periodic with period $\pi/2$ and therefore by expanding in Fourier series, $\alpha(\phi)$ may be written in the form

$$\alpha(\phi) = \alpha_0 + \phi + \alpha_1 \sin(4\phi + \beta_1) + \alpha_2 \sin(8\phi + \beta_2) + \cdots \tag{A15}$$

The expression above gives the phase angle α of the radiated field (with ϕ and r fixed) as a function of the geometrical angle of observation ϕ. In the case of a satellite spinning clockwise about the Z-axis ϕ can be taken as*

$$\phi = 2\pi f_s t \equiv \omega_s t \tag{A16}$$

where f_s is the spin frequency of the satellite, and ω_s is the radian spin frequency. Then (15) becomes

$$\alpha = \alpha_0 + \omega_s t + \alpha_1 \sin(4\omega_s t + \beta_1) + \alpha_2 \sin(8\omega_s t + \beta_2) + \cdots \tag{A17}$$

*Taking the electromagnetic field of a rotating system to be identical to that of a fixed system implies the neglect of the field caused by mechanical motion of charges. This is permissible at low spin rates.

The one-way frequency shift resulting from this phase variation with time will be given by

$$f_1 = \frac{1}{2\pi}\frac{d\alpha}{dt} \tag{A18}$$

$$= f_s + 4f_s\alpha_1 \cos(4\omega_s t + \beta_1) + 8f_s\alpha_2 \cos(8\omega_s + \beta_2) \cdots$$

Equation (18) represents an addition to the Doppler shift already present because of the motion of the satellite in its orbit. The first term is a constant bias equal to the spin frequency, while the succeeding terms represent fluctuations at the 4th, 8th, etc. harmonic of the spin frequency.

The absence of other harmonics is a direct result of the symmetry assumed. If, for example, the feeding currents I_1 and I_2 were not equal, then, referring to (A4) and (5), there would occur in place of (A9) and (A10) the results

$$E_\theta(\phi + \pi) = -E_\theta(\phi) = E_\theta(\phi)e^{j\pi} \tag{A19}$$

$$E_\phi(\phi + \pi) = -E_\phi(\phi) = E_\phi(\phi)e^{j\pi} \tag{A20}$$

and all even harmonics could appear in equation (A18). Complete lack of symmetry, of course, would result in the appearance of odd harmonics.

Simple examples of antenna patterns obtained with specific values of current distributions are given in the following sections.

Pattern of a Small Turnstile Antenna

A general expression for the field of a turnstile antenna is given in Appendix A, equations (A7) and (A8). If the antenna is small, i.e., if the length ℓ of each monopole is small compared to the wavelength, then the currents on the monopoles can be assumed to be approximately linear:

$$f(x) = 1 - \frac{x}{\ell} \quad . \tag{A21}$$

Substituting this function into (A7) and (A8) in the four integrals, approximating each of the four cosine functions by one minus one half the square of its argument, and performing the indicated integration, there results, after some algebraic manipulation

$$E_\eta \doteq -jB\cos\theta\, e^{j\phi}\,[1 - 3b - b\cos 4\phi + jb\sin 4\phi] \tag{A22}$$

$$E_\phi \doteq B\, e^{j\phi}\,[1 - b + b\cos 4\phi - jb\sin 4\phi] \tag{A23}$$

where

$$B \equiv I_1\,\eta k \ell\, e^{-jkr}/4\pi r \tag{A24}$$

and

$$b \equiv k^2 \ell^2 \sin^2\theta/48. \tag{A25}$$

Since $b << 1$ for $\ell << \lambda$, this can be put in the approximate polar form

$$E_\theta = B\cos\theta(1 - 3b - b\cos 4\phi)\, e^{j\left(-\frac{\pi}{2} + \phi + b\sin 4\phi\right)} \tag{A26}$$

$$E_\phi = B(1 - b + b\cos 4\phi)\, e^{j(\phi - b\sin 4\phi)} \tag{A27}$$

The phase angles of the components of the electric intensity agree with the general form (A15).

Pattern of a Very Small Turnstile Antenna with Unbalance Feed

The equations (A4) and (A5) give the field of a turnstile antenna fed by currents I_1 and I_2. If the turnstile is very small, the currents on the monopoles may be assumed, as in the section above to be given by equation (A21), and each integral in (A4) and (A5) is approximately equal to $\ell/2$ since each of the four cosine factors under the integral signs is approximately unity. With the further assumption that the feeding currents are not quite equal

$$\frac{|I_2|}{|I_1|} = q \approx 1 \tag{A28}$$

but are in quadrature

$$I_2 = j\,q\,I_1 \,. \tag{A29}$$

The field of the antenna becomes approximately

$$E_\theta = B\cos\theta\left(1 + \frac{q-1}{2} - \frac{q-1}{2}\cos 2\theta\right) e^{j\left(-\frac{\pi}{2} + \phi + \frac{q-1}{2}\sin 2\phi\right)} \tag{A30}$$

$$E_\phi = B\left(1 + \frac{q-1}{2} + \frac{q-1}{2}\cos 2\phi\right) e^{j\left(\phi - \frac{q-1}{2}\sin 2\phi\right)} \tag{A31}$$

where B is given by (A24).

As expected, in this case the phase pattern

$$\alpha(\phi) = \phi - \frac{q-1}{2}\sin 2\phi \tag{A32}$$

of E_ϕ exhibits a non-zero value of the second harmonic.

CONCLUSIONS

The general conclusion to be drawn from equation (A18) and from the example (A32) is that the one-way Doppler between the satellite and the ground station will be modified by the satellite spin with a constant bias equal to the spin rate* and by fluctuations at harmonics of the spin rate. Because of the electrical and physical symmetry of the antenna system, the fourth eighth, etc. harmonics should be substantial. The size of the 2nd, 6th, etc. harmonics depends on how well the symmetry between the two antenna parts of the system is maintained in practice. Also, unless perfect symmetry exists, the fundamental and odd harmonics should be present to some small degree.

As noted in the introduction, the satellites Explorer 33 and 35 actually employ for tracking a two-way Doppler system in which transmission and reception

*This possibility has been reported in the literature (Reference 11).

occur at different frequencies over the same antenna system. The system is balanced for transmission, and may be expected to exhibit some lack of balance for reception. The exact effect of such an arrangement on the amplitude of the bias and fluctuations depends on the frequency ratios and antenna connections used, and will be discussed in detail in a future report. The value of the bias will, however, be roughly the same as for the one-way case if the antenna connections are such that the spin frequency shift introduced in the uplink signal adds to the shift imparted to the downlink signal. For example, if the spin rate f_s is 1/2 cycle per second, then, assuming an approximate value of 2 meters for the VHF wavelength of the carriers, a range rate bias as large as $(1/2) \times 2 =$ 1 meter per second could be obtained. The antenna connections used on Explorers 33 and 35, however, are such that the frequency shifts caused by the satellite spin in the uplink and downlink signal tend to cancel each other, and the net bias introduced is more than an order of magnitude smaller than the value of 1 meter per second given above.

The frequency of fluctuations introduced by the spin, however, is the same as for one-way Doppler, no matter what connections are used.

APPENDIX B

Method of Analysis

For each data stretch, the following computations were performed.

A least squares straight line $\overline{T}$ was fitted to the data, T_i ,

$$\overline{T} = a_0 + a_1 i, \qquad (B1)$$

$$(i = 1, 2, \cdots n)$$

and residuals, r_i , from this straight line,

$$r_i = T_i - \overline{T}_i \qquad (B2)$$

were then analyzed for their spectral content.*

Letting Δt be the time interval between adjacent values r_i, mean lagged products C_k , with lag interval $\Delta t = h\Delta t$, were calculated.

$$C_k = \frac{1}{n - hk} \sum_{q=0}^{n-hk} r_q r_{q+hk} \qquad (B3)$$

$$\left(k = 0, 1, \ldots, m, m \leq \frac{n}{h}\right).$$

Raw spectral density estimates V_k were obtained next.

$$V_k = \Delta\tau \left[C_0 + 2 \sum_{q=1}^{m-1} C_q \cos\left(\frac{qk\pi}{m}\right) + C_m \cos(k\pi) \right] \qquad (B4)$$

$$(k = 0, 1, \ldots, m)$$

*This particular method for obtaining the spectral density can be found in The Measurement of Power Spectra by R. B. Blackman and J. W. Tukey (reference 12).

Finally, refined spectral density estimates U_k were calculated.

$$U_1 = 1.08\, V_1 + 0.92\, V_2$$

$$U_m = 1.08\, V_m + 0.92\, V_{m-1} \qquad \text{(B5)}$$

$$U_k = 0.46\, V_{k-1} + 1.08\, V_k + 0.46\, V_{k+1}$$

$$(k = 2,\ 3,\ \ldots,\ m - 1)\,.$$

Frequency Aliasing

If a periodic function, say, $\cos(2\pi f t)$, is sampled at equally spaced intervals of time $\Delta\tau$, the following values of the function are obtained.

$$g(i) = \cos(2\pi f\, i\, \Delta\tau) \qquad \text{(B6)}$$

$$(i = \ldots -2,\ -1,\ 0,\ 1,\ 2,\ \ldots)\,.$$

A sampling interval of $\Delta\tau$ seconds gives rise to a maximum resolvable (cutoff) frequency of $f_c = (1/2\Delta\tau)$ cycles/second. Letting $f = nf_s$ be a harmonic of the satellite spin rate f_s, $g(i)$ can be written

$$g(i) = \cos(2\pi n f_s\, i\, \Delta\tau) \qquad \text{(B7)}$$

$$= \cos\left[(2\pi)(2)(k/2\Delta\tau)\, i\, \Delta\tau \pm 2\pi n f_s\, i\Delta\tau\right]$$

$$= \cos\left\{\pm 2\pi\left[(2kf_c - nf_s)\, i\, \Delta\tau\right]\right\}$$

$$(k = 1,\ 2,\ \ldots)$$

$$(i = \ldots -1,\ 0,\ 1,\ \ldots)$$

$$(n = 1,\ 2,\ 3,\ \ldots)$$

From B7 we see that for $|2kf_c - nf_s| \leq f_c$, the frequencies $|2kf_c - nf_s|$ and nf_s $(k = 1, 2, \ldots)$ are indistinguishable and are called aliases of each other.

APPENDIX C

The Standard Deviation Of An Estimated Parameter In A Least Squares Non-Linear Regression Model*

Let $\hat{z}$ be an $(n\times 1)$ vector of measurements of some variable such as two-way Doppler data, x a $(k\times 1)$ vector of parameters, and $z(x)$ an $(n\times 1)$ vector of computed values of the model which we assume adequately describes the observed data. We wish to determine that value x^* of x which minimizes

$$Q = (\hat{z} - z(x))^T (\hat{z} - z(x)) \tag{C1}$$

where the symbol T indicates the transpose, and $k < n$.

For Q to be minimized, it is necessary that the gradient of Q with respect to x, evaluated at $x = x^*$, vanish. Differentiating (C1)

$$F(x) = \nabla_x Q = -2A^T(\hat{z} - z(x)) \tag{C2}$$

where

$$A = \left(a_{ij} = \frac{\partial z_i}{\partial x_j}\right) = A(x) \text{ is an } (n \times k) \text{ matrix of rank } k < n$$

By neglecting the dependence of A on x, we can use a modified Newton-Raphson iteration technique to find a solution x^* such that $F(x^*) = 0$. (See Figure C-1 for a graphical representation of the Newton-Raphson technique in one dimension.) Differentiating (C2) gives

$$F'(x) = \nabla_x^2 Q = 2A^TA. \tag{C3}$$

The second derivative in (C3) is always positive definite (since A was assumed to have rank $k < n$). Therefore, if the process converges to x^*, Q will be minimized.

---

*This development can be found in Reference 13.

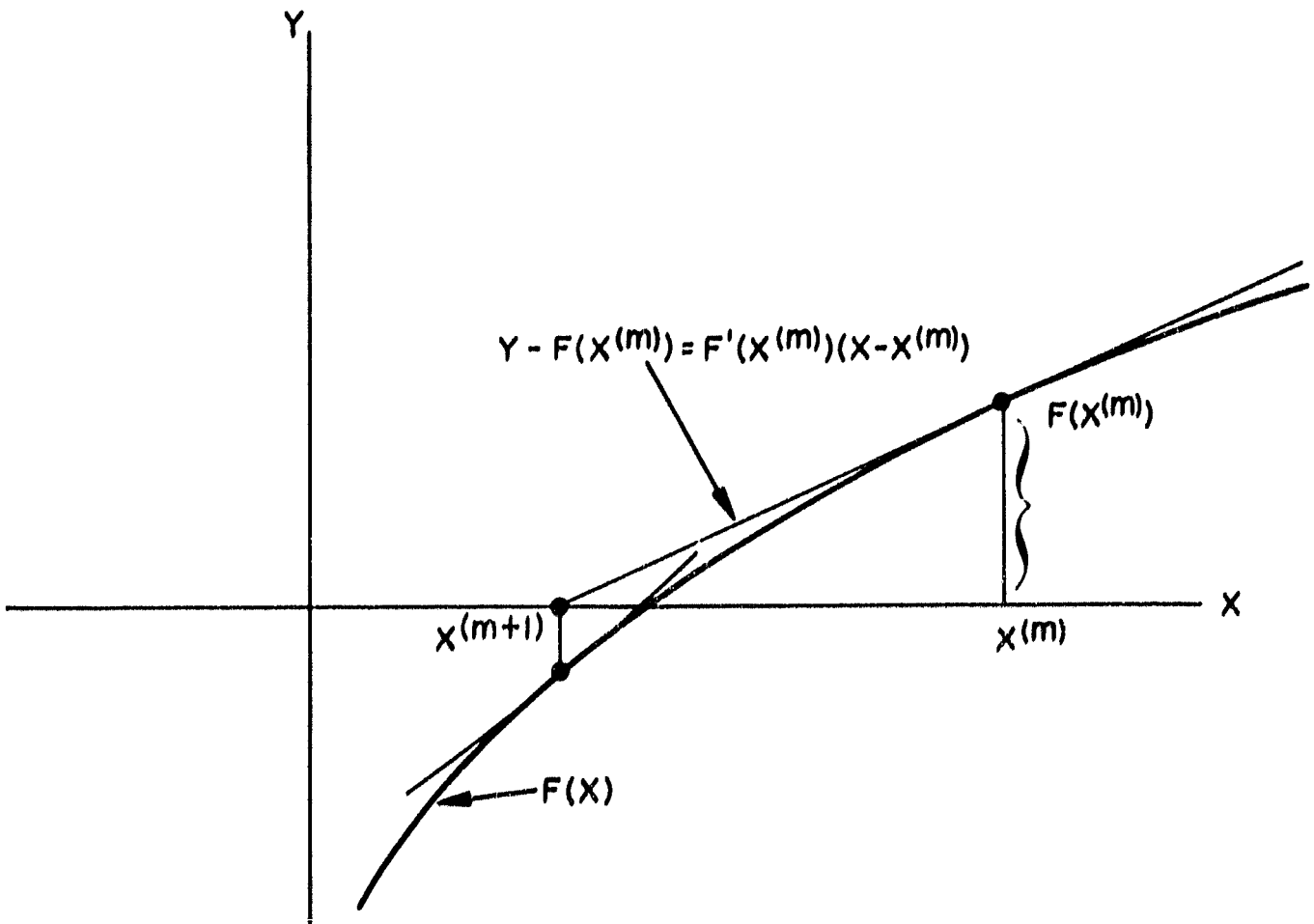

SOLUTION AT $(m+1)^{TH}$ ITERATION

$$X^{(m+1)} = X^{(m)} - \frac{F(X^{(m)})}{F'(X^{(m)})}$$

NASA-GSFC-TBDS
MISSION & TRAJECTORY ANALYSIS DIVISION
BRANCH MSAB DATE 2/6/69
BY C.W. MURRAY, Jr. PLOT NO.

Figure C1–Newton-Raphson Iteration Technique in One Dimension

Denote by $x^{(m)}$ the estimate of the solution at the m^{th} iteration. Then, the "improved" estimate $x^{(m+1)}$ is

$$x^{(m+1)} = x^{(m)} + (A^T A)^{-1} A^T (\hat{z} - z(x^{(m)})) \tag{C4}$$

where

$$A = A(x^{(m)}).$$

Letting $\Delta x = \Delta x^{(m+1)} = (x^{(m+1)} - x^{(m)})$ and $\Delta z = \Delta z(x^{(m)}) = (\hat{z} - z(x^{(m)}))$, we can rewrite (C4) as a "correction" to be applied at the $(m+1)^{th}$ iteration.

$$\Delta x = (A^T A)^{-1} A^T \Delta z \tag{C5}$$

where $(A^T A)^{-1}$ is the inverse of $(A^T A)$.

Equation (C5) shows how small measurement errors (measured minus calculated) propagate through the assumed model in the neighborhood of the least squares solution $x^* = x^{(m+1)}$. In other words, by neglecting the dependence of A on x, the error model indicated in (C5) becomes linear in the neighborhood of $x^* = x^{(m+1)}$.

Now let ΔZ be a random vector representing the error in the measured values $\hat{z}$ from the calculated least squares values $z(x^*)$ (the residuals) and ΔX a random vector representing the error in x due to ΔZ. We will assume that ΔZ has an expected value and covariance matrix given by

$$\begin{aligned} &\mathcal{E}(\Delta Z) = 0 \\ &\mathcal{E}((\Delta Z)(\Delta Z)^T) = \sigma^2 I . \end{aligned} \tag{C6}$$

where I is the $(n \times n)$ identity matrix.

By (C6), we are assuming that the measurement errors are uncorrelated, have zero means and common variance σ^2.

For the Goddard Range and Range Rate Tracking System, the sampling rates are less than the minimum bandwidth of the noise (10 Hz, reference 5). Therefore, if we have modeled the data adequately, having removed all deterministic trends, just "noise" with the properties in (C6) should remain.

Writing (C5) in random vector notation gives

$$\Delta \mathbf{X} = (\mathbf{A}^T \mathbf{A})^{-1} \mathbf{A}^T \Delta \mathbf{Z}. \tag{C7}$$

From (C7) $\Delta \mathbf{X}$ has expected value and covariance matrix,

$$\mathcal{E}(\Delta \mathbf{X}) = 0$$

$$\mathbf{P} = \mathcal{E}(\Delta \mathbf{X} \, \Delta \mathbf{X}^T) = \sigma^2 (\mathbf{A}^T \mathbf{A})^{-1}. \tag{C8}$$

Since we do not know σ^2, we must estimate it from the sample of residuals. Therefore,

$$\mathbf{P} \doteq s^2 (\mathbf{A}^T \mathbf{A})^{-1} \tag{C9}$$

where

$$s^2 = \left(\frac{1}{n - k} \right) (\hat{\mathbf{Z}} - \mathbf{Z}(\mathbf{X}^*))^T (\hat{\mathbf{Z}} - \mathbf{Z}(\mathbf{X}^*)) \tag{C10}$$

and

$$\mathbf{X}^* = \mathbf{X}^{(m+1)}$$

is an unbiased estimate of σ^2 in the neighborhood of $\mathbf{X}^*$ where (by C5) the error model is linear (see reference 14 for the least squares estimator in the linear model).

Therefore, the standard deviation $\sigma_{x_i^*}$ of X_i^* (X_i^* is one of the k components of $\mathbf{X}^*$) from (C9) is to a good approximation given by

$$\sigma_{x_i^*} \doteq \sqrt{P_{ii}} \tag{C11}$$